Multiscale Variational Modeling and Characterization of Materials and Structures

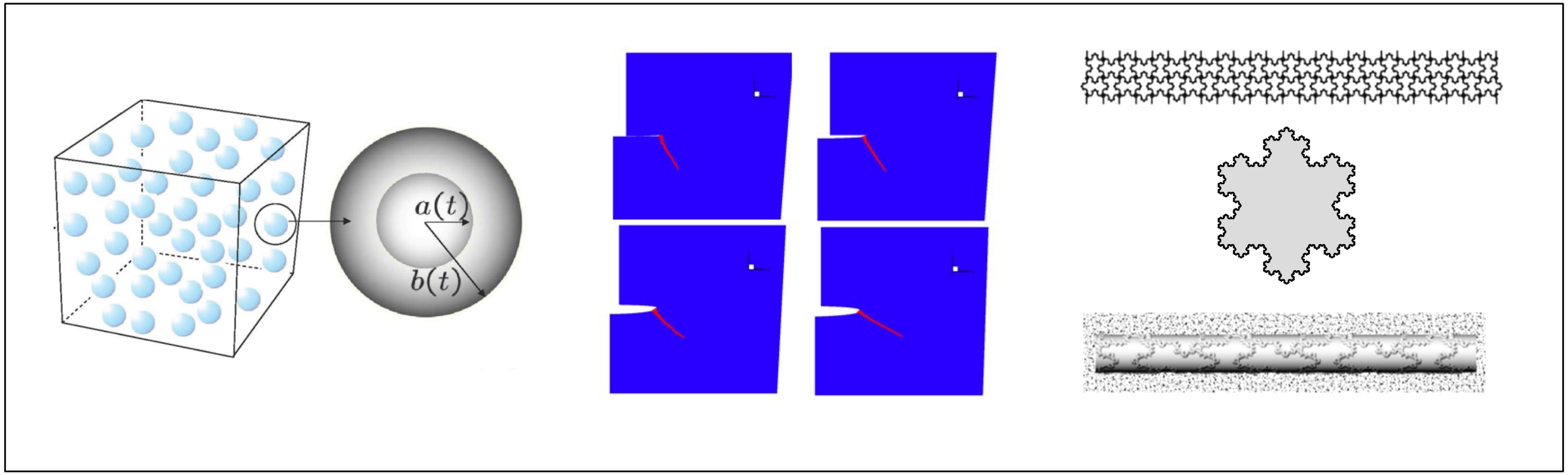

Fernando Fraternali

Department of Civil Engineering University of Salerno, Italy

Department of Civil Engineering,
KU Leuven, 2 December 2014

Outline

Part I: Multiscale Constitutive Models of Brittle and Ductile Materials

Part II: Experimental Investigations on Recycled Plastic Fiber Reinforced Concretes and Mortars

Part I: Multiscale Constitutive Models of Brittle and Ductile Materials

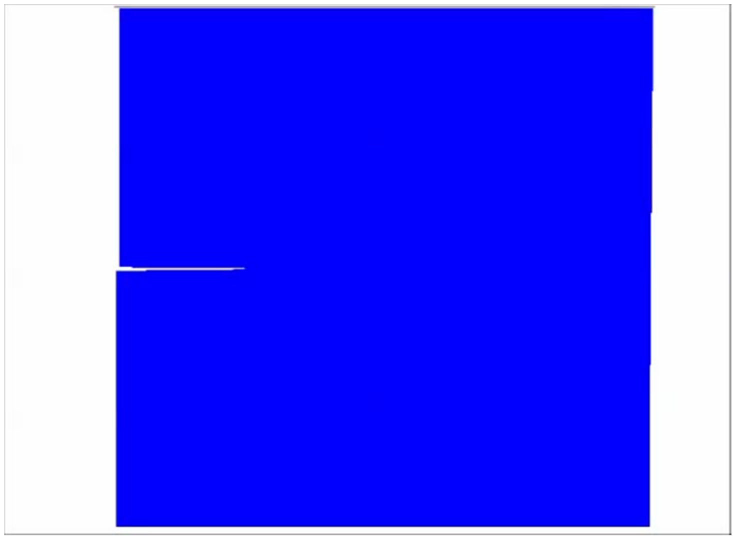

Elsayed, Mota, **Fraternali,.,** Ortiz, **J BIOMECH**, 2008; **COMPUT METHOD APPL M , 2008; COMP MECH**. 2009; Schmidt, **Fraternali,** Ortiz, **MULTISCALE MODEL SIM**, 2009; **Fraternali,** Negri, Ortiz, . **INT J FRACTURE**, 2010; Blesgen, **Fraternali,** Raney, Daraio, **MULTISCALE MODEL SIM**, 2013; **Fraternali,** Carpentieri, Amendola,. **J MECH PHYS SOLIDS**, 2014.

Motivation

- Development of a variational framework including viscoelastic, elastic-plastic and brittle/cohesive models in finite strain kinematics for use in stress analysis, and damage prediction /simulation.

- Covered effects:

  finite deformation kinematics

  shear damage via deviatoric plasticity

  volumetric damage by porous plasticity

  viscous and strain-rate effects

  brittle and cohesive fracture

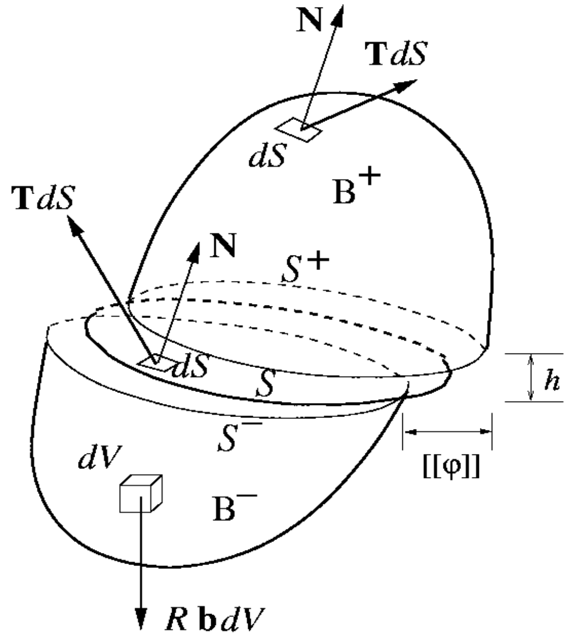

- Response at the meso-scale informed by quasi-continuum simulations

- Constitutive relations discretized in time by recourse to variational updates

- Fracture and shear band damage via mesh-independent localization elements and variational material erosion

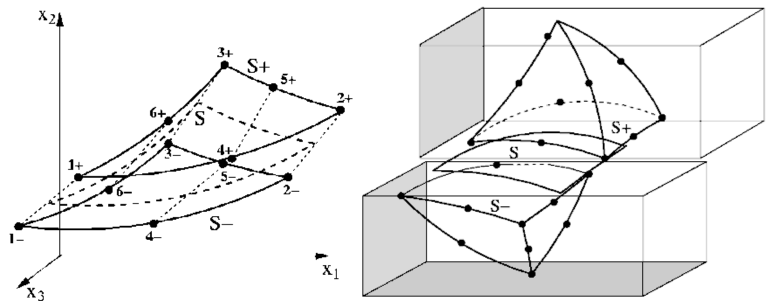

Finite Strain Kinematics

Multiple multiplicative decomposition of the deformation gradient into elastic-plastic and viscoelastic components

$$\boldsymbol{F} = \boldsymbol{F}^e \boldsymbol{F}^p = \boldsymbol{F}^e_1 \boldsymbol{F}^v_1 = \ldots = \boldsymbol{F}^e_M \boldsymbol{F}^v_M$$

M := number of (Maxwell-type) viscous mechanisms

Plastic flow rule

internal variables

Viscous flow-rules

$$\boldsymbol{Z}^p = \{\theta^p, e^p\}$$

$$\dot{\boldsymbol{F}}^p \boldsymbol{F}^{p-1} = \dot{\theta}^p \boldsymbol{N} + \dot{e}^p \boldsymbol{M}$$

$$tr\boldsymbol{M} = 0\ ,\ \boldsymbol{M} \cdot \boldsymbol{M} = \frac{3}{2}\ ,\ \boldsymbol{N} = \pm \frac{1}{3} \boldsymbol{I}$$

$$\dot{e}^p \geq 0\ ,\ \dot{\theta}^p \geq 0$$

$$\boldsymbol{Z}^v_i = \left\{\theta^v_i, e^v_{i,1}, e^v_{i,2}, e^v_{i,3}\right\}$$

$$\dot{\boldsymbol{F}}^v_i \boldsymbol{F}^{v-1}_i = \frac{\dot{\theta}^v_i}{3} \boldsymbol{I} + \sum_{j=1}^{3} \dot{e}^v_{i,j}\ \boldsymbol{M}^v_{i,j} \quad (i = 1, \ldots M)$$

$$\boldsymbol{M}^v_{i,j} \in Sym\ ,\ \boldsymbol{M}^v_{i,j} \cdot \boldsymbol{M}^v_{i,h} = \delta_{jh}$$

Free energy

$$A(\boldsymbol{F}, \boldsymbol{F}^p, \boldsymbol{Z}^p, \boldsymbol{F}_i^v, \boldsymbol{Z}_i^v, T) =$$

$$W^e(\boldsymbol{F}\boldsymbol{F}^{p-1}, T) + W^p(\boldsymbol{Z}^p, T) + \sum_{i=1}^{M} W_i^e(\boldsymbol{F}\boldsymbol{F}_i^{v-1}, T) + \rho_0 C_v T(1 - \log \frac{T}{T_0})$$

First Piola-Kirchhoff stress tensor and thermodynamic forces

$$\boldsymbol{P} = \frac{\partial A}{\partial \boldsymbol{F}}$$

$$\boldsymbol{T}^p = -\frac{\partial A}{\partial \boldsymbol{F}_p} \quad , \quad \boldsymbol{Y}^p = -\frac{DA}{D\boldsymbol{Z}^p}$$

$$\boldsymbol{T}_i^v = -\frac{\partial A}{\partial \boldsymbol{F}^i} \quad , \quad \boldsymbol{Y}_i^v = -\frac{DA}{D\boldsymbol{Z}_i^v}$$

Volumetric plastic damage

Volumetric damage is related to the plastic expansion of spherical voids in a plastically incompressible matrix (N: number of voids per unit volume; a: void radius)

Volumetric expansion:

$$\dot{\theta}^p = \left| \frac{d}{dt} \log J^p \right|, \qquad \theta^p(t) = \theta^p(0) + \int_0^t \dot{\theta}^p(\xi)\, d\xi$$

Voids fraction:

$$f_0 = N \frac{4\pi a_0^3}{3} \qquad J^p = 1 - f_0 + N \frac{4\pi a^3}{3}, \qquad f = \frac{f_0 + J^p - 1}{J^p}$$

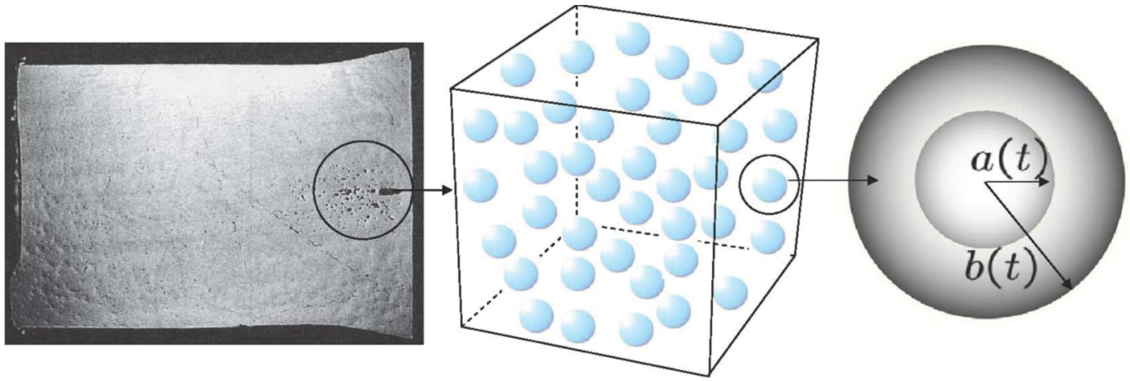

Damage localization **Void distribution** **Void kinetics**

Evolution laws of internal variables: kinetic potentials

$$\dot{\boldsymbol{Z}}^p = \frac{\partial \psi}{\partial \boldsymbol{Y}^p} \quad , \quad \dot{\boldsymbol{Z}}_i^v = \frac{\partial \phi_i}{\partial \boldsymbol{Y}_i^v} \quad (i = 1, ..., M)$$

$$\psi^*(\boldsymbol{F}^p, \dot{\boldsymbol{Z}}^p, T) = \sup_{\boldsymbol{Y}^p} \left\{ \boldsymbol{Y}^p \cdot \dot{\boldsymbol{Z}}^p - \psi(\boldsymbol{Y}^p, \boldsymbol{F}^p, T) \right\}$$

$$\phi_i^*(\boldsymbol{F}_i^v, \dot{\boldsymbol{Z}}_i^v, T) = \sup_{\boldsymbol{Y}_i^v} \left\{ \boldsymbol{Y}_i^v \cdot \dot{\boldsymbol{Z}}_i^v - \phi(\boldsymbol{Y}_i^v, \boldsymbol{F}_i^v, T) \right\} (i = 1, ..., M)$$

$$\boldsymbol{Y}^p = \frac{D\psi^*}{D\dot{\boldsymbol{Z}}^p} \quad , \quad \boldsymbol{Y}_i^v = \frac{D\phi_i^*}{D\dot{\boldsymbol{Z}}_i^v}$$

Incremental constitutive updates with variational structure

$$W_k(\boldsymbol{F}_{k+1}, T_{k+1}) =$$

$$\min_{\boldsymbol{Z}^p_{k+1}, \boldsymbol{M}, \boldsymbol{N}, \boldsymbol{Z}^v_{i,k+1}, \boldsymbol{M}^v_{i,j}} D_k(\boldsymbol{F}_{k+1}, T_{k+1}, \boldsymbol{Z}^p_{k+1}, \boldsymbol{M}, \boldsymbol{N}, \boldsymbol{Z}^v_{i,k+1}, \boldsymbol{M}^v_{i,j})$$

$$D_k(\boldsymbol{F}_{k+1}, T_{k+1}, \boldsymbol{Z}^p_{k+1}, \boldsymbol{M}, \boldsymbol{N}, \boldsymbol{Z}^v_{i,k+1}, \boldsymbol{M}^v_{i,j}) =$$

$$W^e(\boldsymbol{\epsilon}^e_{k+1}, T_{k+1}) + W^p(\boldsymbol{Z}^p_{k+1}, T_{k+1}) +$$

$$\sum_{i=1}^{M} W^e_i(\boldsymbol{\epsilon}^e_{i,k+1}, T_{k+1}) + \rho_0 C_v T_{k+1}\left(1 - \log\frac{T_{k+1}}{T_0}\right) +$$

$$\Delta t\left(\psi^*_{k+1} + \sum_{i=1}^{M} \phi^*_{i,k+1}\right) + \beta \Delta t^2 B_{k+1}$$

void
microinertia

$$\Delta t = t_{k+1} - t_k$$

Variational theory of fracture

Fracture as a free discontinuity problem

$$\min_{(\boldsymbol{\varphi},K)\,\in\,A(\bar{\boldsymbol{\varphi}}(t))}\left\{E(t)\;(\varphi,\,K)\;=\int_{\Omega\setminus K}W(\boldsymbol{X},\nabla\boldsymbol{\varphi}(\boldsymbol{X}))\;d\boldsymbol{X}\right.$$

$$\left.-\int_{\Omega\setminus K}F(t,\boldsymbol{X},\boldsymbol{\varphi}(\boldsymbol{X}))\;d\boldsymbol{X}-\int_{\partial_S\Omega}G(t,\boldsymbol{X},\boldsymbol{\varphi}(\boldsymbol{X}))\;d\mathcal{H}^{n-1}(\boldsymbol{X})\right\}$$

$$+\int_K\vartheta\left(\boldsymbol{X},\delta\left([\![\boldsymbol{\varphi}]\!](\boldsymbol{X}),\boldsymbol{\nu}(\boldsymbol{X})\right)\right)\;d\mathcal{H}^{n-1}(\boldsymbol{X})\Big\}$$

Weak formulation in SBV spaces

$$\min_{\boldsymbol{\varphi}\,\in\,\mathcal{A}(\bar{\boldsymbol{\varphi}}(t))}\;\{I(t)(\boldsymbol{\varphi})\;=\;E(t)(\boldsymbol{\varphi},J_{\boldsymbol{\varphi}})\}$$

Eigenfracture model

Use of mesh-independent, variational fracture models («Eigenfracture», cf. *Schmidt, B,* ***Fraternali, F.,*** *Ortiz, M. Eigenfracture: An Eigendeformation Approach to Variational Fracture. MULTISCALE MODELING & SIMULATION, 7 (3), 1237-1266, 2009*) to predict time-evolution of fracture damage in brittle and cohesive solids, with special attention to masonry structures.

Eigenfracture energy functional: $\int_\Omega W(\mathcal{E}u-\gamma) + \frac{G}{2\varepsilon}\underbrace{|\{\gamma \neq 0\}_{h,\varepsilon(h)}|}$,

ε-neighborhood of the cracked region ($\gamma \neq 0$).

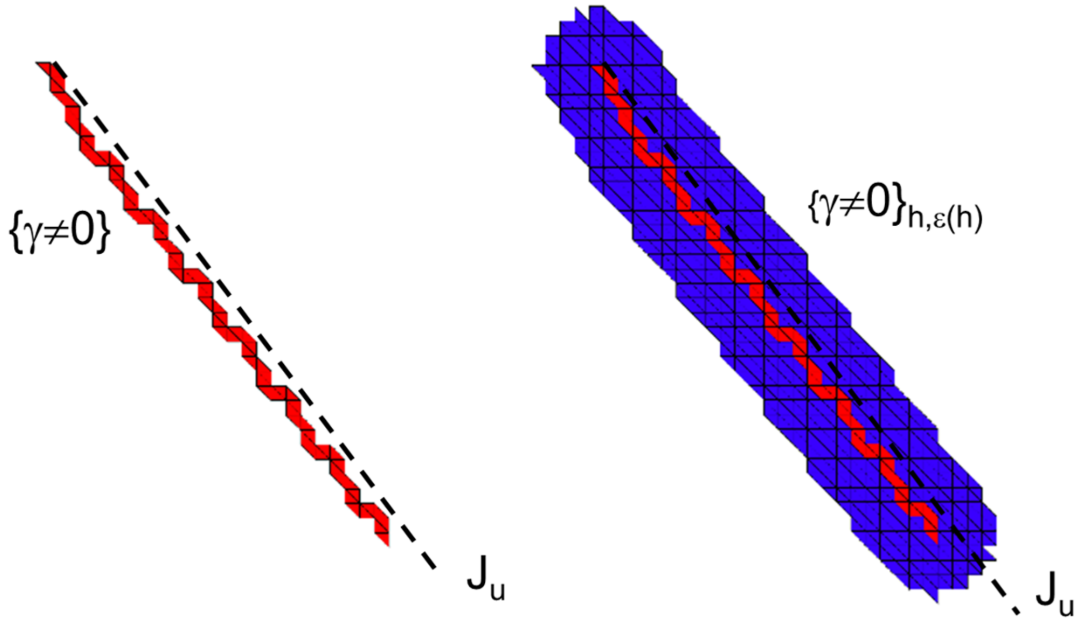

Notice that $|(\gamma\neq 0)|$ DOES NOT CONVERGE to the measure of limiting crack set $|J_u|$, while

$1/2\ \varepsilon\ |(\gamma\neq 0)_{h\ ,\ \varepsilon(h)}|$

CONVERGES to $|J_u|$.

Correction of mesh dependency

Quasi-static fracture simulation

Mixed modes I-II:

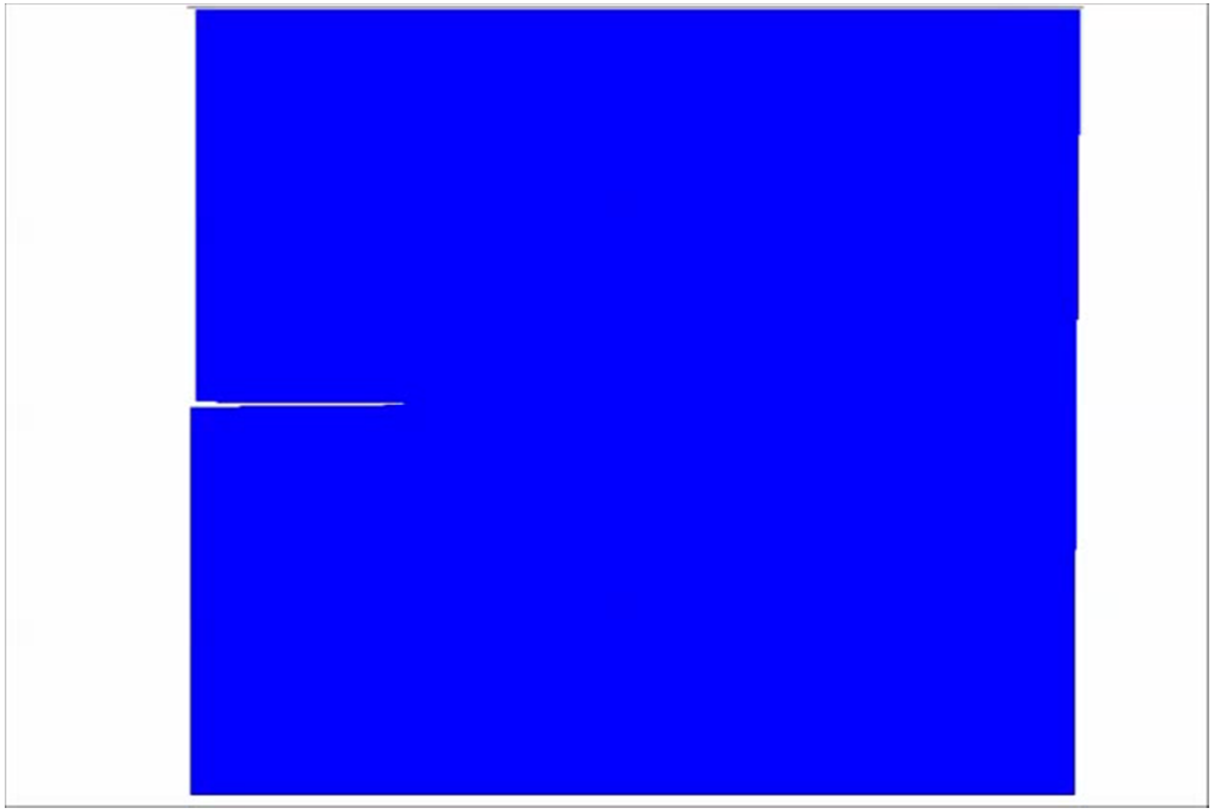

material erosion along the crack path

Prediction of fracture damage in masonry structures

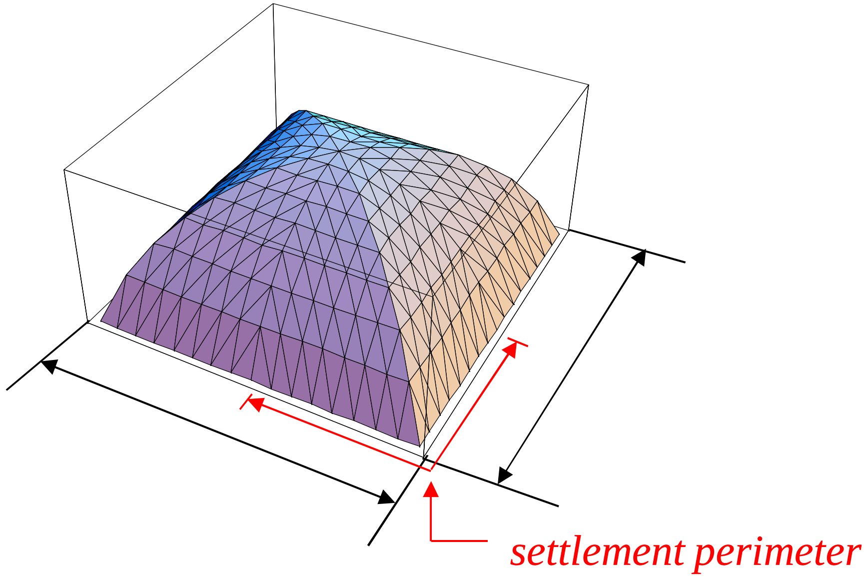

Real-scale model

Experimental crack pattern

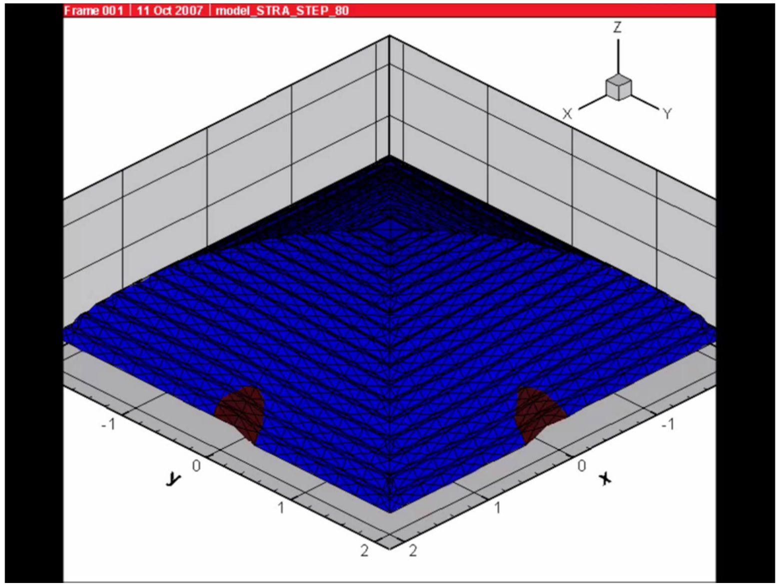

Eigenfracture prediction

Prediction of collapse mechanisms of unreinforced and reinforced masonry structures

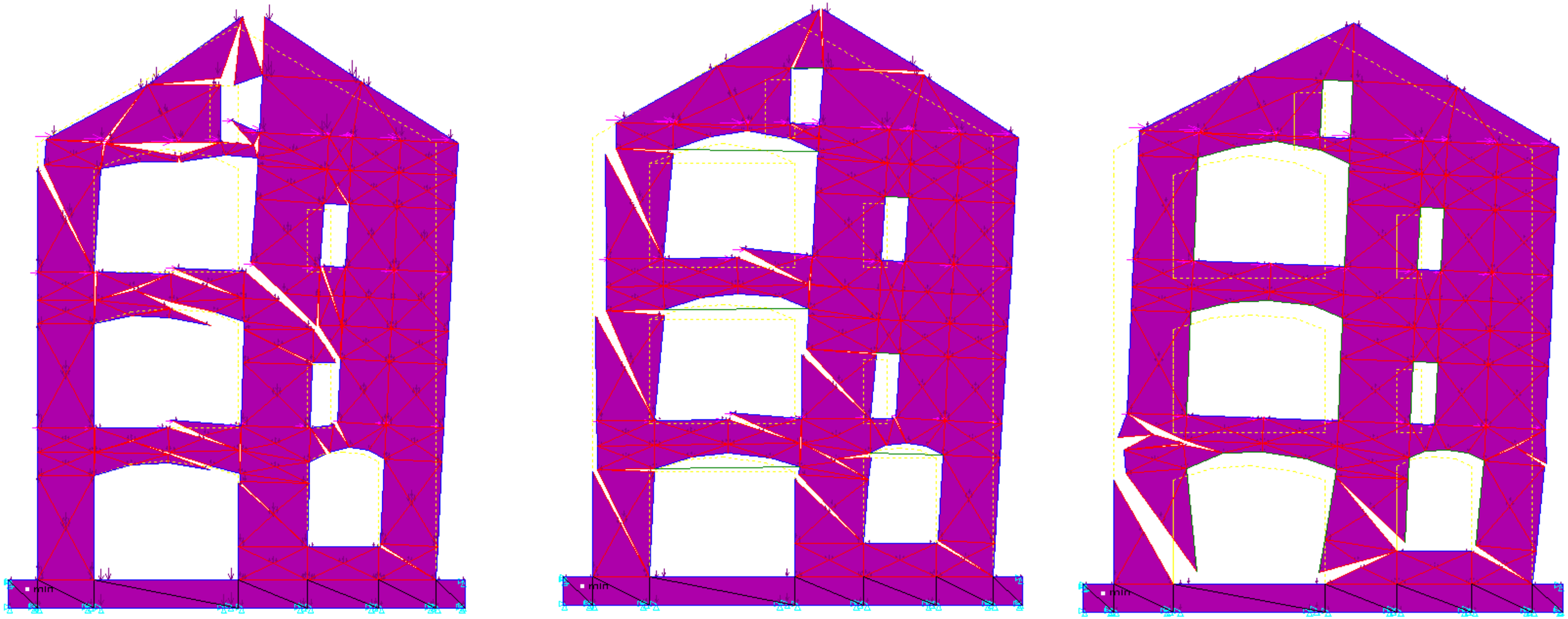

Unreinforced masonry

$\lambda_c = 3.9827$

Masonry reinforced with steel ties and flitched beams

$\lambda_c = 6.2945$

FRP/FRG/SRG-reinforced masonry

$\lambda_c = 9.2505$

Part II: Experimental Investigations on Recycled Plastic Fiber Reinforced Concretes and Mortars

Fraternali, Ciancia, Chechile, Rizzano, Feo, Incarnato, **COMPOS STRUCT**, 2011; **Fraternali,** Farina, Polzone, Pagliuca, Feo, **COMPOS PART B-ENG**, 2013; **Fraternali,** Spadea, Berardi, **CONSTR BUILD MATER**, 2014; Spadea, Farina, Berardi, Dentale, **Fraternali, ING SISM**, 2014.

Motivation

Building trades are great contributors to environmental degradation.

Reduce the environmental impact of the construction process.

Innovative materials.

Concrete reinforcement with aggregates and/or fibers obtained from waste plastics

Concrete/mortar reinforcement with recycled plastic fibers

Low-cost technique for the enhancement of:

- Thermo-acoustic insulation properties
- Compressive/Tensile strength
- Fracture toughness
- Structural ductility

Materials

- Recycling post-consumer PET bottles

Plastic fibers were produced by mean a of R-PET flake extrusion lines available in the plants of the Techno Plastic (TP) S.r.l. of Castelfranco Emilia (Modena, Italy) and FHP S.a.s. – Plastic Division of Roncello (Milan, Italy), two world leader companies in the sector of plastic monofilament extrusion. The production process comprises the following phases: crystallization, drying, pneumatic transportation, dosing, extrusion, filtering, spinning, stretching, stabilization, winding, polywrapping, and fiber cutting.

Materials

- Recycled PET fibers and concrete mix-design

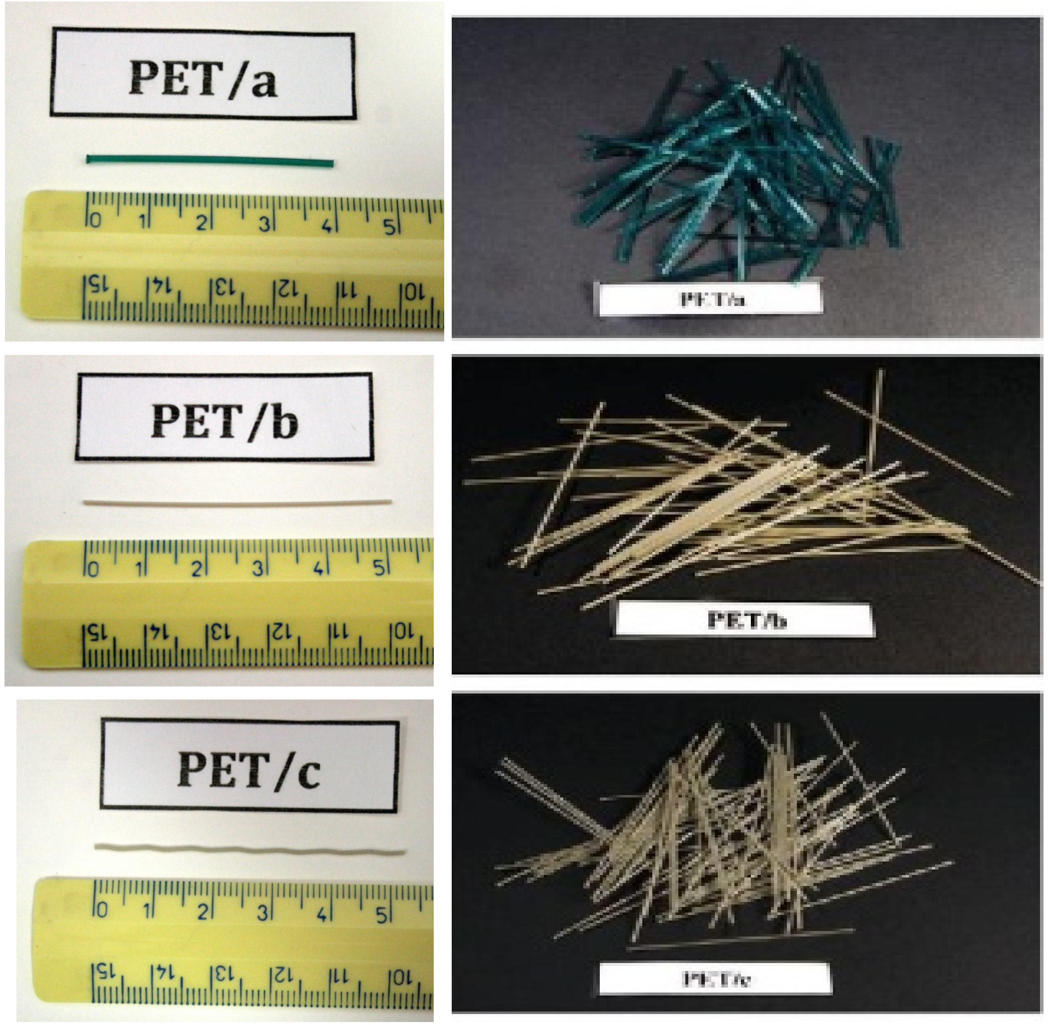

Component	Dosage (Kg/m^3)
Pozzolanic Cement CEM IV/B 32.5 R	340
Water/Cement ratio (%)	53

Property	PET/a	PET/b	PET/c	PP
Specific gravity	1.34	1.34	1.34	0.90
Cross section	Circular	Circular	Circular	Oval
Aspect	Straight	Straight	Crimped	Embossed
Diameter (*mm*)	1.10	0.70	0.70	0.80 × 1.30
Lenght (*mm*)	40	52	52	47
Tensile strenght (*MPa*)	550.00	263.72	274.29	250.00
Ultimate strain (%)	27	26	19	29

Materials

- Fiber mixing

Experimental results - 1

- Thermal conductivity

Material	k (W/mK)	95% CI (W/mK)	FRR (%)
UNRC	0.967	0.284	0.0
RPETFRC/a	0.793	0.251	-18.0
PPFRC	0.756	0.139	-21.8

- Compressive strength

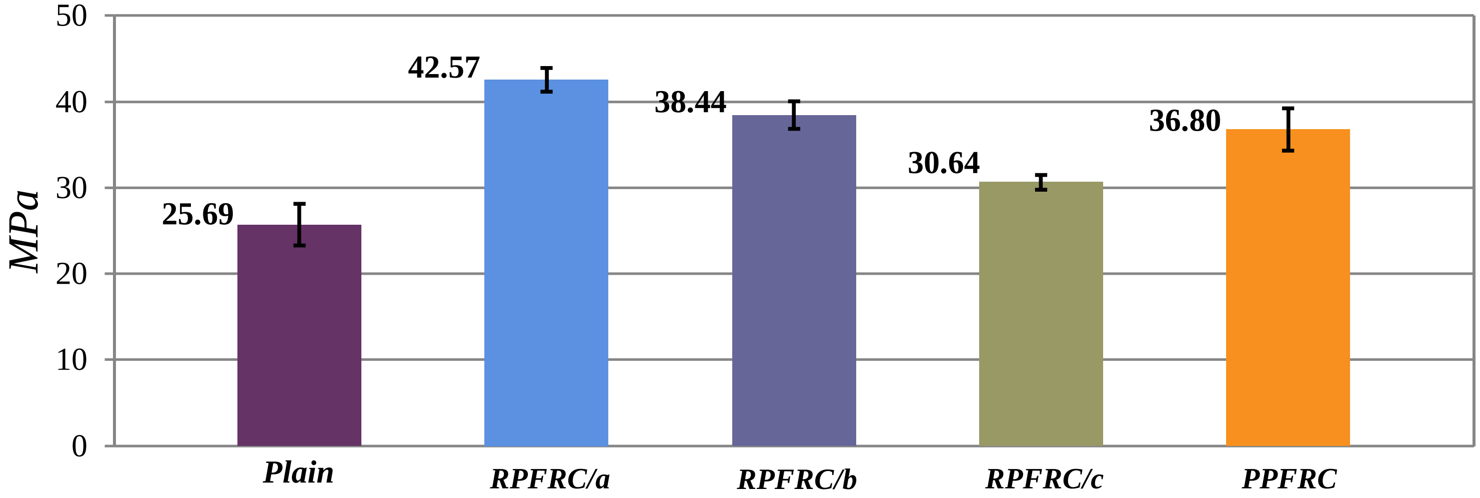

Experimental Results - 2

- First crack strength and ductility indices

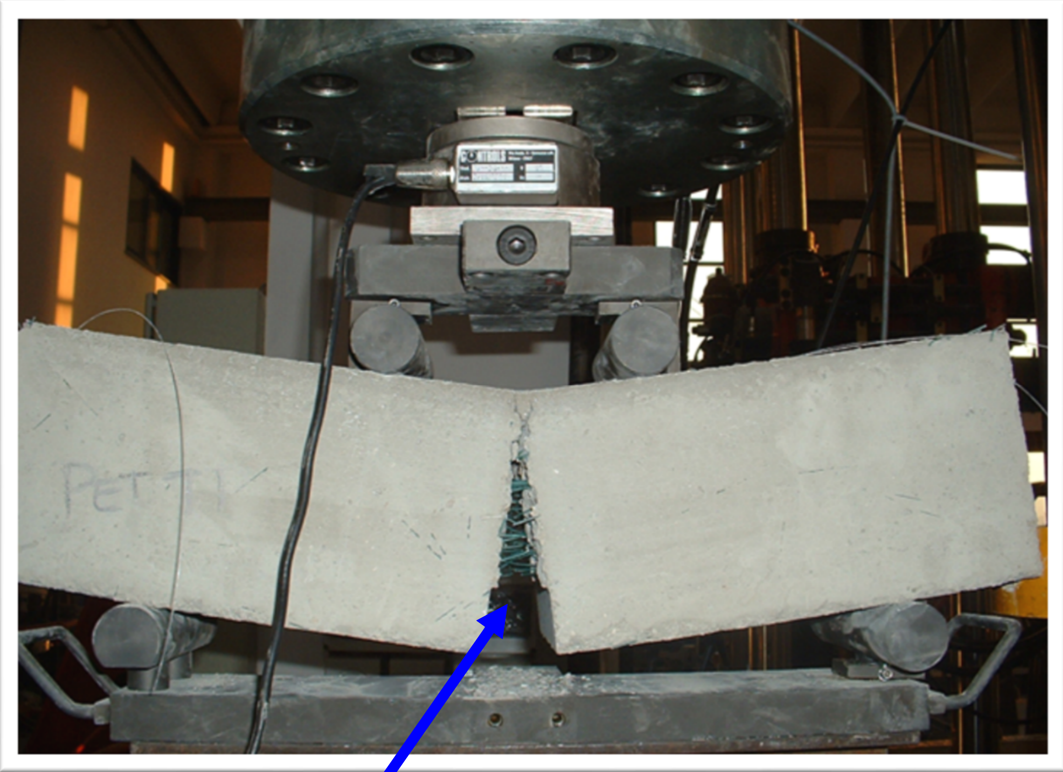

bridging effect

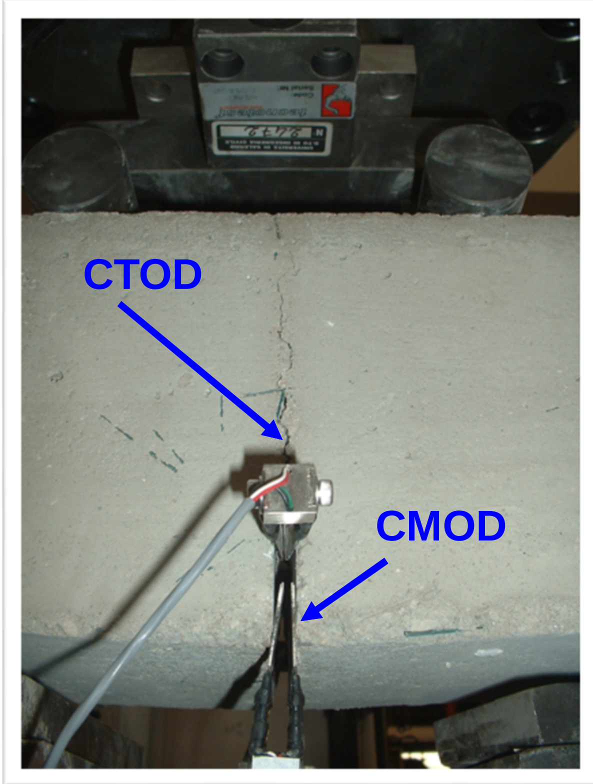

Experimental Results - 3

- Force-CTOD plots

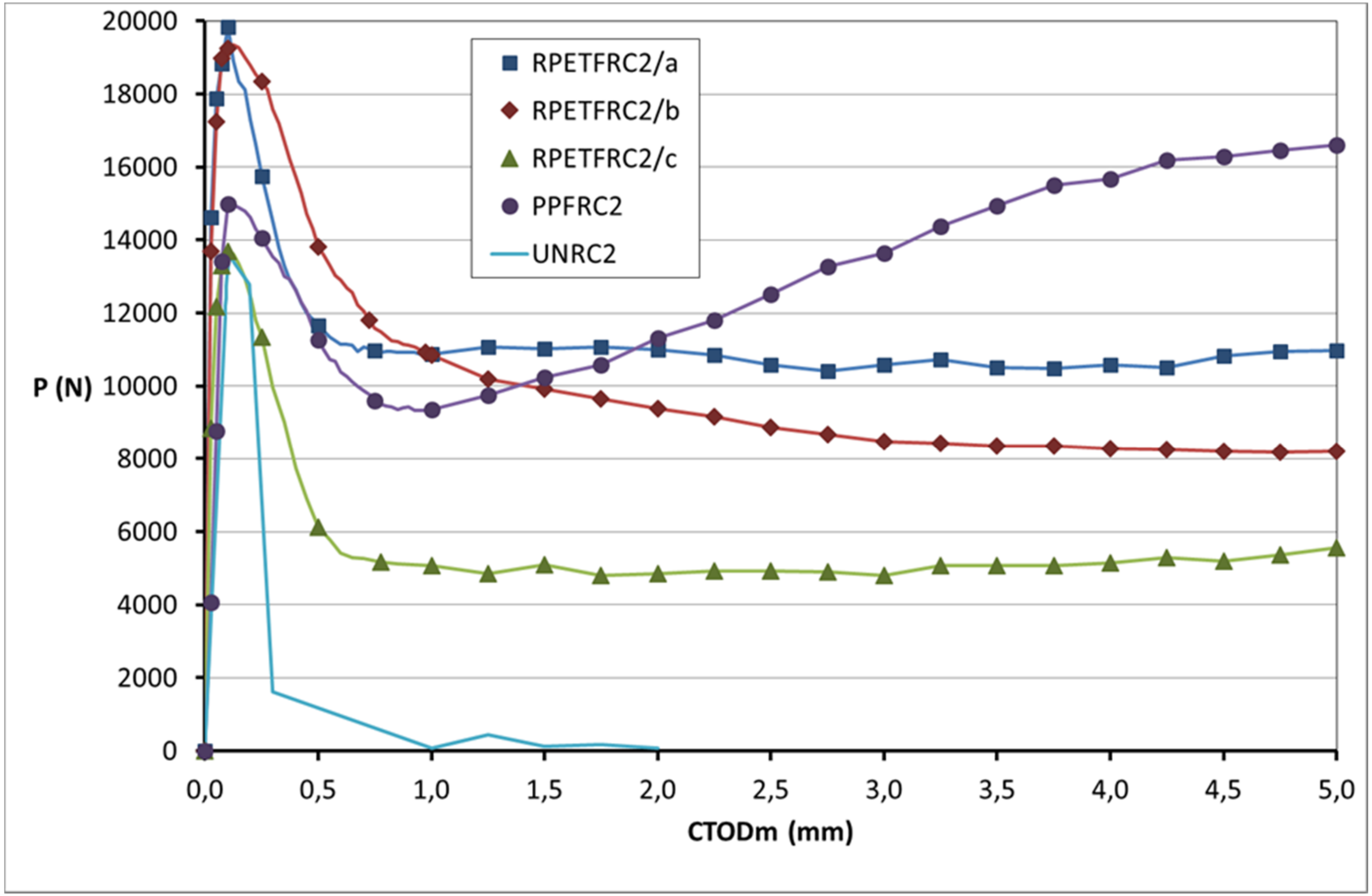

Seawater curing of RPETFRC

- Force-CTOD plots

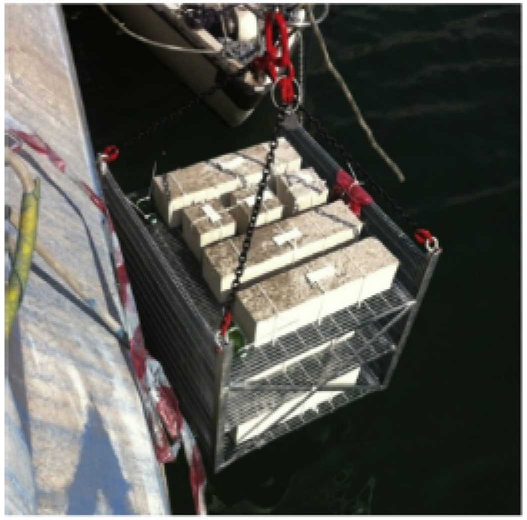

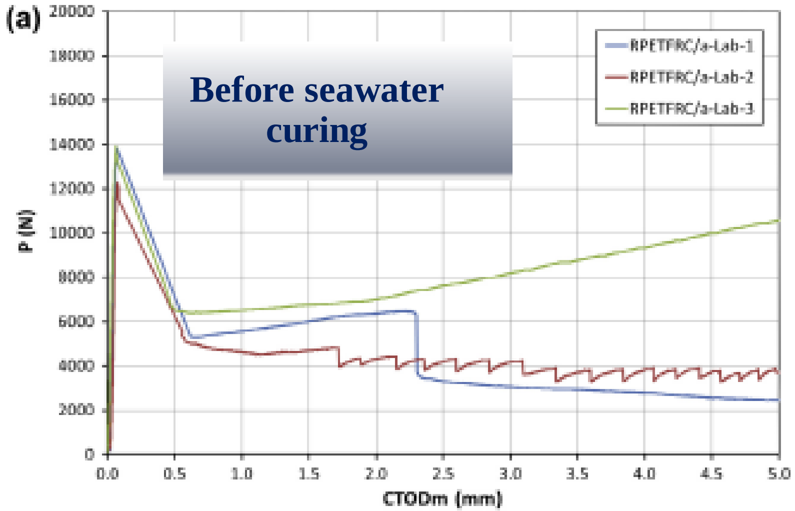

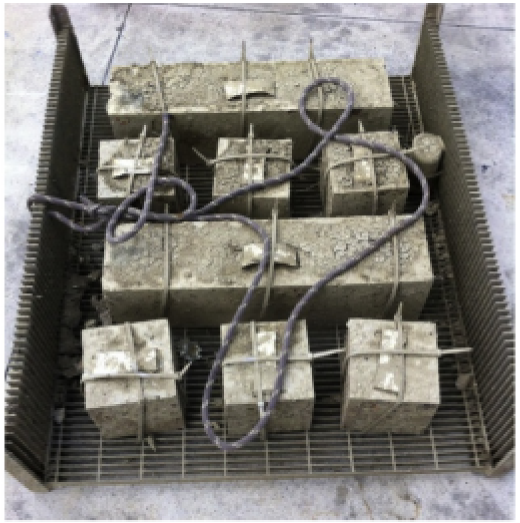

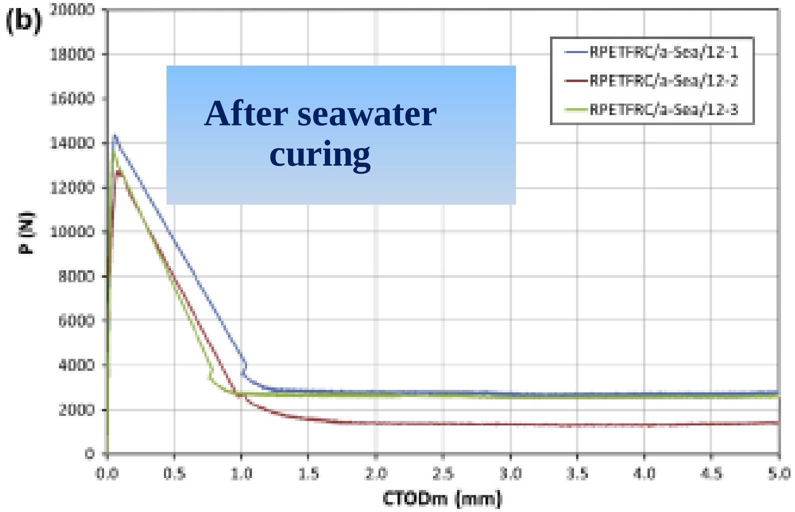

R-PET reinforcement of cementitious mortars

- Manual cutting of R-PET strips
- Force-deflection plots

7 days curing

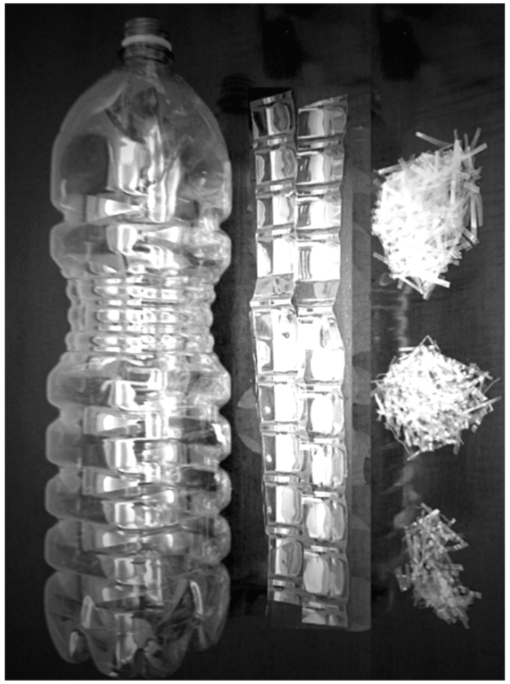

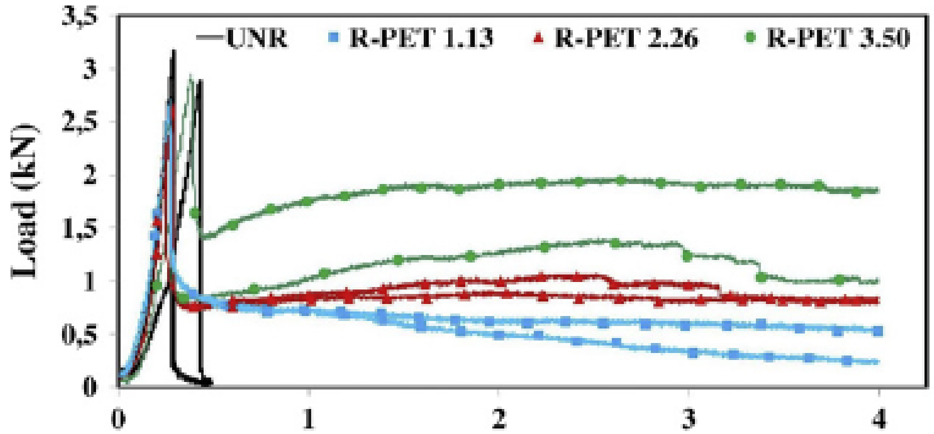

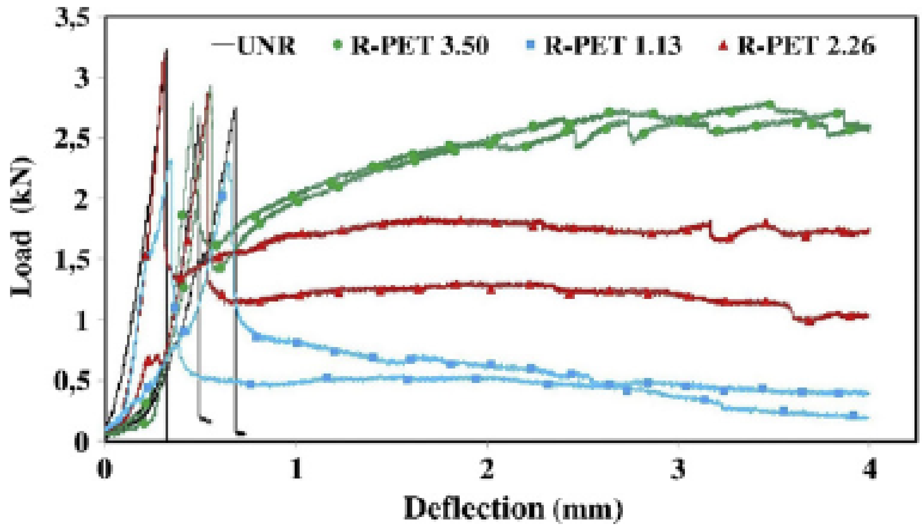

28 days curing

R-Nylon reinforcement of cementitious mortars

- Recycling fish poaching nets

- Force-deflection plots

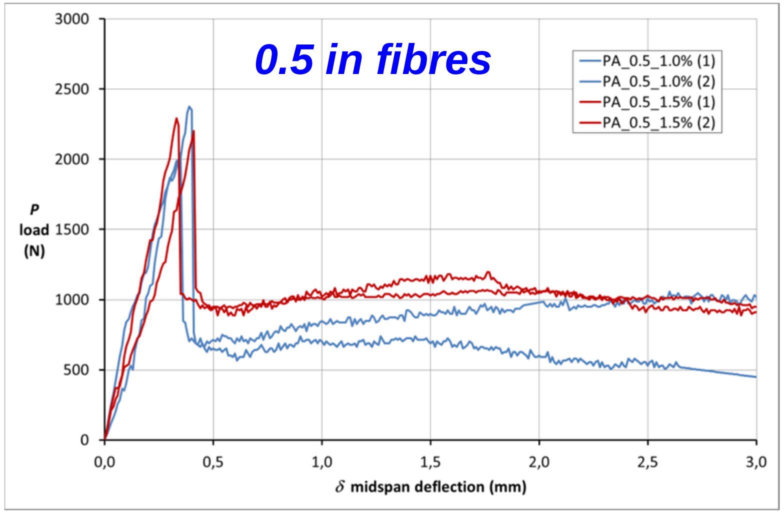

- First-crack strength

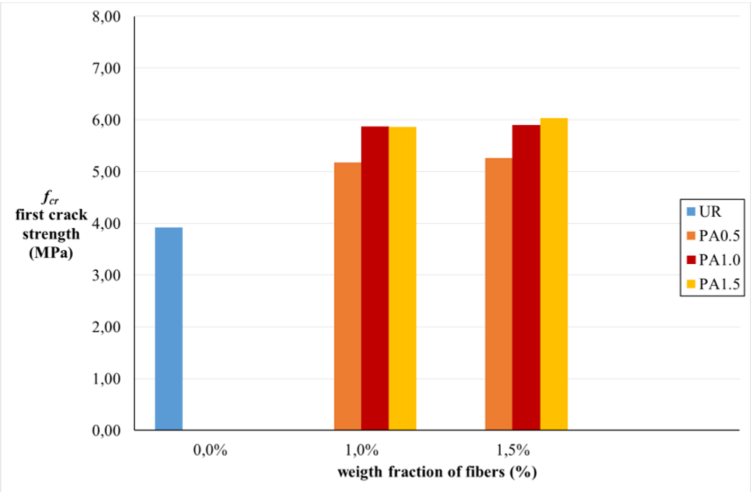

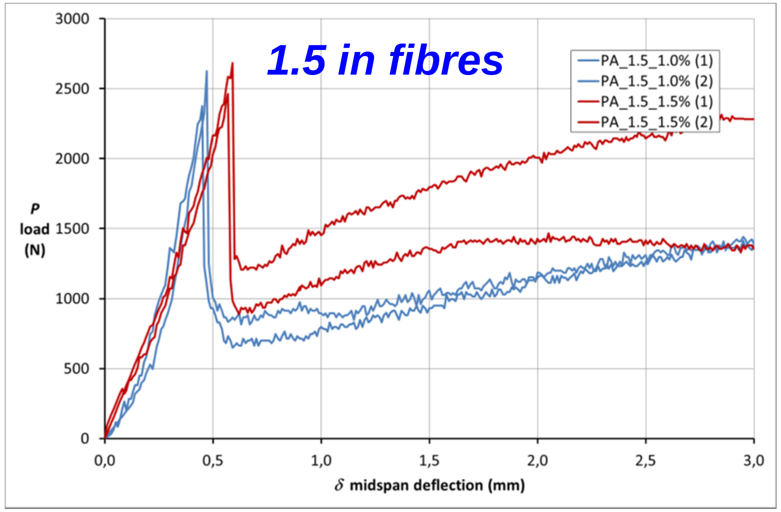

CONCLUSIONS

Marked improvements of all the examined therrmo-mechanical properties of RPETFRC in the case of a pozzolana cement based concrete with 0.53 water/cement ratio.

Fiber reinforcement with *PET/a*

- Compressive strength, +35**%**
- First crack strength, +**41%**
- Ductility index D0, +**16%**
- Ductility index D1, +**656%**

Fiber reinforcement with *PET/c*

- Compressive strength, +**20%**
- First crack strength, +**8%**
- Ductility index D0, +**16%**
- Ductility index D1, +**545%**

Fiber reinforcement with *PP*

- Compressive strength, +**44%**
- First crack strength, +**10%**
- Ductility index D0, +**30%**
- Ductility index D1, +**700%**

Other observed results:

- reduction of compressive and first-crack strengths with the water/cement ratio
- high strength fibers (PET/a) are the most beneficial in the case of low water/cement ratio
- crimped fibers (PET/a) are the most beneficial in the case of low water/cement ratio
- seawater curing does not significantly affect first-crack strength , but markedly reduce the energy absorption capacity

FUTURE WORK:
Multiscale mechanical modeling of heterogeneous materials

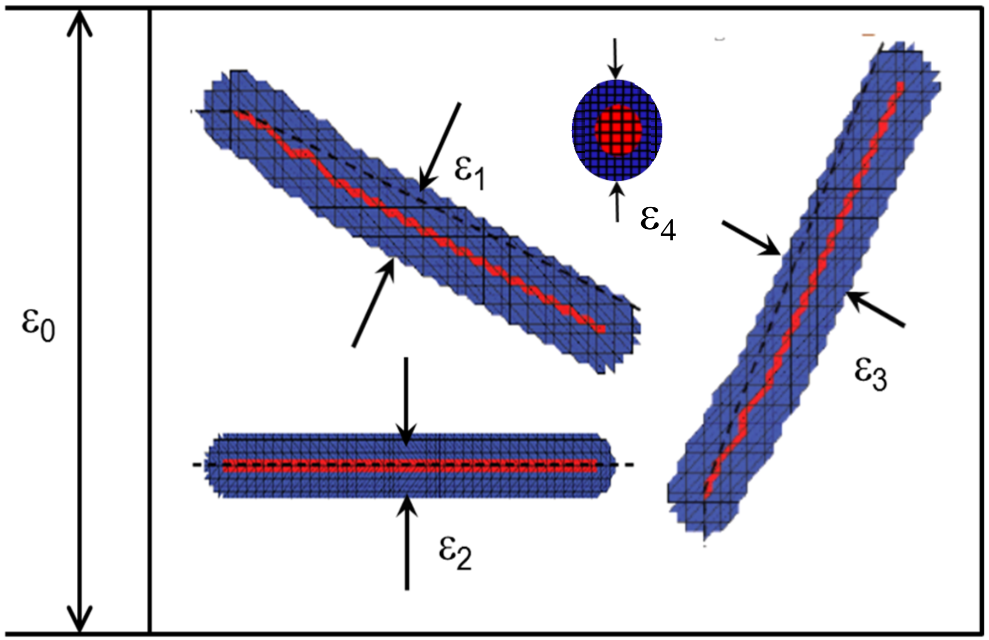

Multiscale modeling of composite materials (such as, e.g., concretes, fibre-reinforced and particulate composites, etc.) based on the Gamma-converge of energy functionals depending on multiple scale factors; bulk energies of the different phases; and interface energies due to micro-cracking (via eigenfracture).
Study of the composite mechanic response; creep phenomena; synergic effects in hybrid fiber composites; blended binders cementitious materials for conservation practices, etc..